ARCHIVES OF ACOUSTICS
22, 1, 85–92 (1997)

CLASSIFICATION OF ACOUSTIC EMISSION SIGNALS REGISTERED DURING THE FOAM DRAINAGE PROCESS

Z. RANACHOWSKI and P. RANACHOWSKI

Institute of Fundamental Technological Research
Polish Academy of Sciences
(00-049 Warszawa, ul. Świętokrzyska 21)

This article refers to the changes of spectral features of Acoustic Emission (AE) signal. The AE signal is generated during drainage process concerning a foam made of detergent solution. The subroutines to extract the AE events and its spectral features from the real AE signal recordings are described. The effectiveness of classifying procedures based on two linear and one nonlinear algorithms used to recognition different AE patterns is also discussed.

1. Generation of Acoustic Emission during the foam drainage process

In this paper the changes of spectral features of an AE signal generated by the foam formed from the liquid phase are described. The theoretical model of this effect was presented in [1, 2]. The foam investigated in this article was made during a local pressure fluctuation processes occuring when the liquid detergent was poured into the experimental vessel. The movement of the detergent resulted in the formation of a population of bubbles on the surface of the liquid. The diameters of the bubbles gradually increased. The multiphase complex described above tended to achieve a dynamic equilibrium in approx. 15–20 min. after the foam formation. During this process, beside the bubble diameter increase, a thinning of the bubble walls caused by the drainage and a gradual approach of the bubble junctions to the walls of the experimental vessel was observed. The thinning of the bubble walls led to collapsing and incorporation of the weakest structures while the AE signal was generated. It was evaluated in [3] that the mechanically excited bubbles behave as resonant vibrators with specific pulsation ω_0:

$$\omega_0^2 \approx \frac{3\gamma P_e}{\varrho R^2}, \tag{1}$$

where γ – ratio of the specific heat under constant pressure to that at constant volume, P_e – pressure of the bubble in the absence of vibrations, ϱ – specific density of the medium surrounding the bubble, R – diameter of the bubble at the equilibrium between external and internal pressures.

The pressure of the bubble depends of its diameter R and the pressure of the surrounding medium P_0 according to the Laplace's formula:

$$P_e = P_0 + 2\sigma/R, \tag{2}$$

where σ – surface tension of the bubble coat.

In the investigations described a 0.142 M/dm^3 solution of the nonionic detergent, Triton X – 100 was applied, which stabilizes the foam composition. The structure of the detergent molecule is presented in Fig. 1.

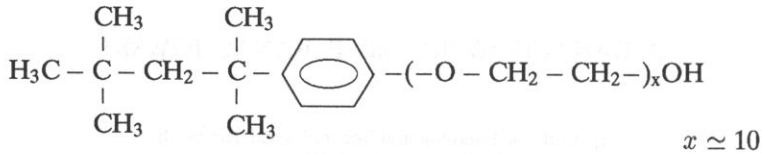

Fig. 1. The structure of the detergent molecule used in the investigation.

The procedure of generation of the foam was similar to that used in the Ross-Miles test for foaming properties of surfaces [4]. The experimental found amount of the detergent (9.4 ml) was pouring from the height of 400 mm to the 55 mm diameter glass test-tube. A small broadband sensor of type Nano 30, Physical Acoustic Corp. was glued to the external surface of the test-tube. The AE signals were amplified and high-pass-filtered (over 20 kHz) using a EA200 Acoustic Emission Processor, made at the Institute of Fundamental Technological Research. An IWATSU DS 6612C storage oscilloscope was connected to the output of the AE processor to capture the AE waveforms. When the amplitude of the AE signal (after 93 dB amplification) was greater than 1 V, the trigger of the oscilloscope enabled the capturing of 2 miliseconds of the AE signal at a sampling rate of 500 kHz. More than 700 of such waveforms were stored in the disk logged in a PC computer applying the procedure described above.

2. Classification of the recorded AE waveforms

The authors of the papers concerning the strategies of the processing of AE signal generated at the presence of the liquid phase [5–7] recommend AE signal descriptors derived in the frequency domain as an efficient signal characterization method. Therefore, the following procedure was applied to determine the different classes of the recorded signals, caused by separate phases of the drainage process. AE waveforms were registered in 50 bytes and formed after Fourier transformation 25 bytes long feature vectors, where the consecutive bytes corresponded to the power of the signal within the 10 kHz band. Thus the entire feature vector covered the 250 kHz band of the registered spectra.

During recording the AE waveforms it was found that the AE activity fades and reaches the noise level after approx. 1000 seconds after the initiation of the process. According to this, the following scheme was used to generate feature vectors corresponding to the different phasees of the investigated process:

1. ten real 25-byte vectors were averaged to form the average feature vector,

2. the first averaged vector was formed of the signals registered within the first 100 seconds of the process, the one was formed of the signals registered within the next 100 seconds of the process, the third vector corresponded with the signals registered within the period 200–300 seconds after the beginning of the process and the fourth one within 400–600 seconds after the beginning of the process,

3. the reference noise vector was formed of the signals recorded after 1000 seconds of the process,

4. the intensity of the signal related to the 10 kHz spectral bands was discretized in such way as to obtain 8 intensity levels, corresponding to the 3 db signal increase,

5. the certain averaged signal level was confirmed by registering its ocurrence in more than 50% averaged vectors.

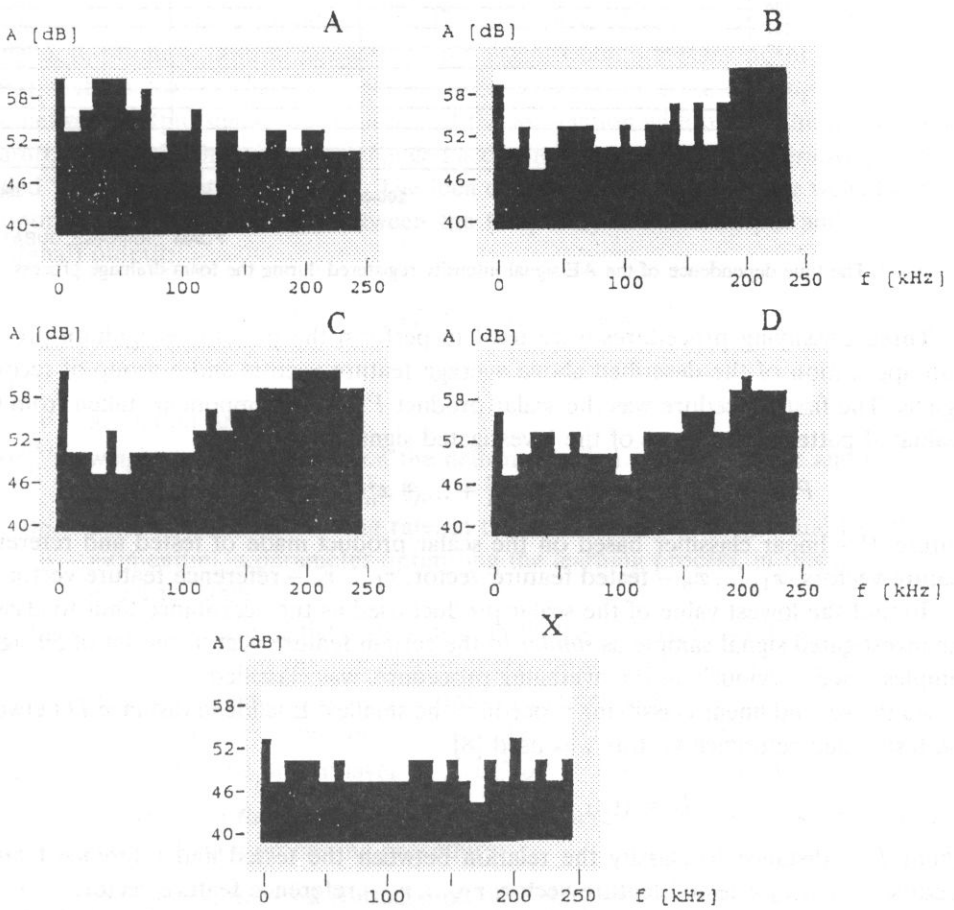

Fig. 2. Four binary average feature vectors reflecting four (A, B, C, D) phases of the drainage process and the average noise feature vector (X).

The four binary average feature vectors, labelled A, B, C, D and the reference average noise feature vector, labelled X, are shown in Fig. 2. The comparison of the image of the

consecutive vectors let us to conclude that at the beginning of the foam drainage process the lower frequencies, probably generated by the collapsing of the largest bubbles, are dominant. In the next periods higher frequencies are registered. During the final signal decrease the high frequency domination was continued. The time dependence of the AE signal intensity, evaluated with the use of the averaged feature vectors described above, is shown in Fig. 3.

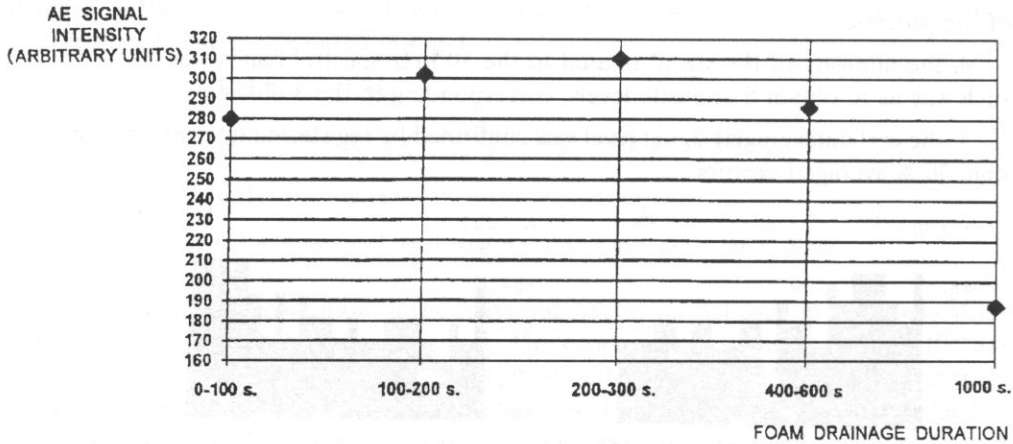

Fig. 3. The time dependence of the AE signal intensity registered during the foam drainage process.

Three classifying procedures were used to perform the pattern recognition process with application of the described above average feature vectors and a group of recored signals. The first procedure was the scalar product P of the components taken from the evaluated patterns and those of the investigated signal samples:

$$P = (x_1 r_1 + \ldots + x_n r_n)/(x_1^2 + \ldots + x_n^2)^{1/2}(r_1^2 + \ldots + r_n^2)^{1/2}, \tag{3}$$

whrere P – linear classifier based on the scalar product made of tested and reference feature vectors, $x_1, \ldots, x_n$ – tested feature vector, $r_1, \ldots r_n$ – reference feature vector.

To find the lowest value of the scalar product used as the acceptance limit to classify the investigated signal sample as *similar* to the certain feature vector, the set of 50 signal samples, used previously in the averaging procedure, was classified.

As the second linear classifying procedure the smallest Euclidean distance D between the tested and reference vectors was used [8]:

$$D = \left((x_1 - r_1)^2 + \ldots + (x_n - r_n)^2\right)^{1/2}, \tag{4}$$

where D – distance to classify the relation between the tested and reference feature vectors, $x_1, \ldots, x_n$ – tested feature vector, $r_1, \ldots, r_n$ – reference feature vector.

To find the highest value of this classifier as the acceptance limit to classify the investigated signal sample as *similar* to the certain feature vector, the set of 50 signal samples was used in the same way as in method (3) described above.

As the third classifying procedure the nonlinear neural network was prepared. Neural network was modelled in the computer memory as the structure consisted of multi-input

vs. single output elements (neurons) connected in several chains called layers [9, 10]. Each neuron output (except the output layer) was connected with all the neurons consisting the next layer. The relation between the element input and output signal for such structures can be expressed as:

$$y_i(t+1) = \theta(\Sigma_j w_{ij} x_j(t) - \mu_i), \tag{5}$$

where $y_i(t+1)$ – neuron output signal after signal processing cycle, θ – neural activation functions (in this paper assumed as $1/(1+\exp(-x))$, w_{ij} – a weighting coefficient which expresses the bonding strength between the connected neurons labelled j and i, $x_j(t)$ – neuron input signal before the signal processing cycle, μ_i – process parameter called threshold level.

The computer model of the neural network consisted of a table of weight coefficients being modified in the learning process. This process was carried out to vary the synaptic weights to obtain a desired network output signal when a certain signal was fed to the input of the network. The aim of the research work presented in this paper was to form the network output signal as a measure of the association with one of the five reference feature vectors. Each weight was changed according to a widely used iterative procedure called "backpropagation of error". The idea of the procedure is to make weight changes proportional to the difference between the temporary network output and the desired (optimal) output:

$$\Delta w_{ij}^{(k)} = \eta_1 (d\theta(E_i)/dE) x_j \sigma_i^{(k)} + \eta_2 m_{ij}^{(k+1)}, \tag{6}$$

where

θ – activation function,
$\Delta w_{ij}^{(k)}$ – weight coefficient between the neuron labelled i in the layer k and the neuron j in the layer $(k-1)$,
η_1 – parameter called learning rate, in this work experimentally equal to 0.01,
η_2 – momentum, a parameter optimising the learning process, in this work equal to 0.008,
E_i – total excitation of the j-th neuron in the layer k, equal to $\Sigma_j w_{ij}^{(k)} x_j$,
z_i – desired signal at the i-th output of the network,
y_i – temporary signal at the i-th output of the network,
m_{ij} – change of the weight coeff. used in the previous iteration,
$\delta_i^{(k)}$ – $z_i - y_i$ for the output layer or $\Sigma_l w_{li}^{(k)} \sigma_l^{(k+1)}$ for the other layers.

For the purpose of the research work described here, the following assumptions have been made for the data processing procedure:

1. the used neural network consisted of 200 binary inputs to analyse the components of the feature vectors,

2. the vector components were analysed in the first layer consisting of 62 neural units,

3. the second layer consisted of five neurons to generate five output signals due to association between the currently analysed vectors and five learned patterns.

3. Comparison of the effectiveness of the classifying methods

The five spectral patterns refferred to the five phases of the foam drainage process were used to compare the effectiveness of the classyfying procedures described in the previous Chapter. The process of classification was performed on five groups of the nine test spectral feature vectors. The latter groups of vectors were preparred as follows. They were derived from the AE signal recorded 25 miliseconds after the signal samples used to form spectral patterns. The idea of this scheme was to obtain the signal samples similar but significantly different with respect to the applied patterns. To find the limit values forming the acceptance ranges to classify the certain vectors to one of the five classes, all the feature vectors once used to form the averaged patterns, were classified. The results of the classification of the test spectral feature vectors by applying the procedure described above are shown in Table 1.

Table 1. The results of the classification of the test spectral feature vectors by applying the three procedures described in Chapter 2.

method of classification	the acceptance range of the classifier	the percentage of succesfully classified vectors
scalar product (Eq. (3))	> 0.85	47 %
Euclidean distance (Eq. (4))	< 6.6	58 %
neural network (Eq. (6))	class A: > 0.225 class B: > 0.171 class C: > 0.206 class D: > 0.165	44 %

Each of the presented methods alone was able to recognize about 50 % of the presented feature vectors. Both linear methods recognized generally the same vectors but the effects of the application of the neural network showed the individual way of classification. Utilizing the neural network method, among the 16 correctly classified vectors of the total population of 36 seven were missed by the linear methods. An example of the differences in the classification process is shown in Fig. 4. The right side of this Figure presents one of the tested vectors of type B (the averaged pattern of this type is drawn on the left side of the Figure). The linear classifiers have recognized this test vector as a type B one. However, in this case, there is some likeness to the types A and C, so the neural network method indicated equal similarity to the three types mentioned.

Important problems related to the propagation of the acoustic emission signal in different media are caused by the attenuation of this signal. Figure 5 presents the averaged pattern of type A (on the left side) and the same pattern after 6 dB attenuation (on the right side). It was proved experimentally that the linear methods were unable to recognize the attenuated feature vector, presented in the described Figure. The same problem was succesfully solved by using the neural network method because the absence of the "traces" of likeness to the concurrent vectors. The ability of the recognition of the vectors derived from weak signals may be explained with respect to the specific signal processing used in the neural network method. The linear methods generate a result

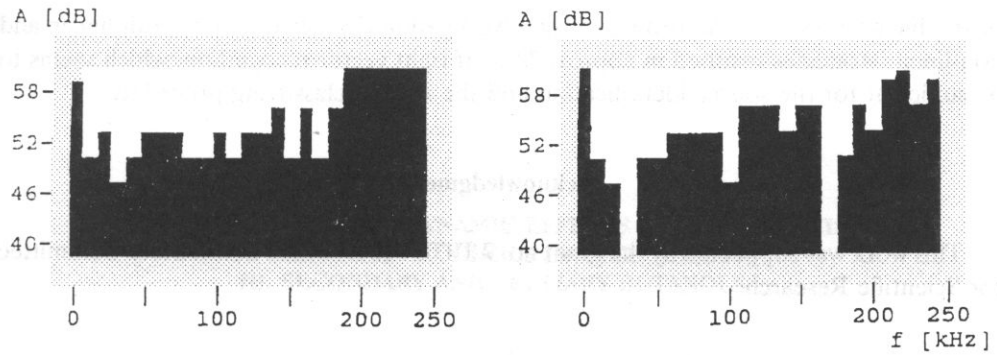

Fig. 4. Binary average feature vector of class B (left) and an example of the member vector of that class succesfully recognized when processed with linear methods and unrecognized when the neural network method was used (right).

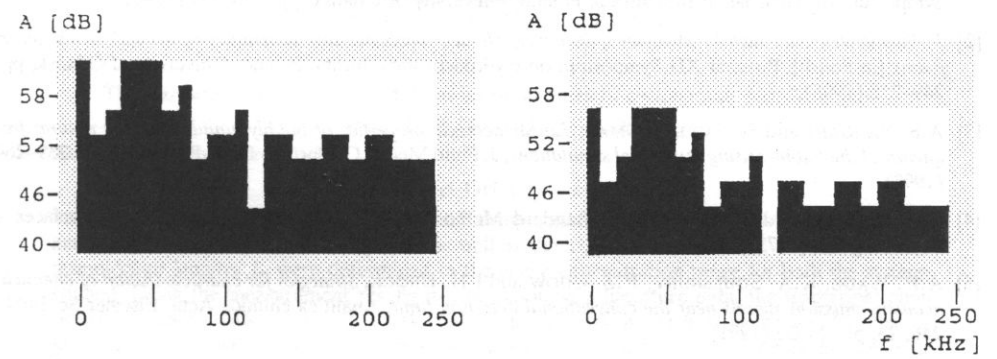

Fig. 5. Binary average feature vector of class A (left) and a modification of this vector after 6 dB attenuation of the Acoustic Emission signal (right).

of comparison increasing the coefficient of likeness for each pair of the fitting elements of the two vectors. The agorithm of the neural network is more complex. Among the positive components forming the likeness coefficient related to the actually processed vector, there are the negative components related to the other memorized vectors.

4. Conclusions

Three methods applicable for classifing the real feature vectors derived from the Acoustic Emission signal were presented in this article. They allow for automatic processing of large sets of signal samples. Each method alone was able to classify correctly about 50 % of processed vectors. According to the assumed criteria, the scalar product method classified 11 % vectors less than the Euclidean distance method.The application of linear methods causes problems of recognition of the weak signals. The neural network method is less effective when there is signifficant likeness of the investigated signal to more than one class. Due to the different classification strategy applied by the neural network method, it is reasonable to use the latter method additionally to one

of the linear classifiers. According to the investigation described above, both linear and non-linear strategies resulted in approx. 78 % of right vector recognition, which seems to be sufficient for the source identification and the related classifying procedures.

Acknowledgment

This work was supported by the grant no. 7 T07B 020 08 of the Polish State Committee for Scientific Research.

References

[1] I. MALECKI and J. RZESZOTARSKA, *Acoustic emission generated by gas bubbles* [in Polish], Proc. of XI Symposium on Hydroacoustics, Jurata, Poland, University of Gdańsk, pp. 320–331 (1994).

[2] J. RZESZOTARSKA and I. MALECKI, *Structure, physical processes and generation of acoustic emission in foams* [in Polish], Proc. of XII Symposium on Hydroacoustics, Jurata, Poland, University of Gdańsk, pp. 249–255 (1995).

[3] A.S. SANGANI and R. SURESHKUMAR, *Linear acoustic properties of bubbly liquids near the natural frequency of the bubbles using numerical simulations*, J. Fluid Mech., Cambridge Univ. Press, 252, pp. 239–264 (1993).

[4] American Standard ASTM 1173-53, Standard Method of Test for Foaming Properties of Surfaces – Active Agents (1973).

[5] A.P. WADE, K.A. SOULSBURY, P.Z. CHOW and I.H. BROCK, *Strategies for characterization of chemical acoustic emission signals near the conventional detection limit*, Analitica chimica Acta, Elsevier Sc. Publ., 246, 23, pp. 23–36 (1991).

[6] C. DELEBARRE, J. FROHLY, I. BAGUET, Z. DEROVICHE and C. BRUNEEL, *Acoustic Signature Estimation of the Cavitation Noise*, Ultrasonics Int. 93 Conf. Proc., Butterworth – Heinemann Ltd, Oxford, pp. 719–723 (1993).

[7] I. MALECKI and J. RANACHOWSKI, *The informatic contents of acoustic emission signals*, Proc. of 15th International Congress on Acoustics, pp. 523–526 (1995).

[8] M. OHITSU and K. ONO, *Pattern Recognition Analysis of Magnetomechanical Acoustic Signals*, J. Acoustic Emission, 3, 2, pp. 69–78 (1984).

[9] J. HERTZ, A. KROGH and R. PALMER, *Introduction to the Theory of Neural Computation*, Addison - Wesley Publ. Comp., Reading Mass. (1991).

[10] R. SRIBAR and W. SACHSE, *AE Source Characterization in Lattice – Type Structures Using Smart Signal Processing*, Ultrasonics Int. 93 Conf. Proc., Butterworth - Heinemann Ltd, Oxford, pp. 221–239 (1993).